at low temperatures.

It is clear that the transport studies of thin films in the QSE region contains a whole wealth of intriguing physical problems, the problem of boundary conditions, the problem of various scattering mechanisms, and the problems associated with the feasible semimetal-semiconductor transition, etc. More accurate measurements in still better vacuum and quantitative-model computations are highly desirable.

ACKNOWLEDGMENTS

We are grateful to Dr. J. M. Dickey for her help in the computer calculation and to O. F. Kammerer for his expert technical assistance.

*Work supported by the U. S. Atomic Energy Commission.

[1]Yu F. Ogrin, V. N. Lutskii, and M. I. Elinson, Zh. Eksperim. i Teor. Fiz. Pis'ma v Redaktsiyu 3, 114 (1966) [Sov. Phys. JETP Letters 3, 71 (1966)]; V. N. Lutskii, D. N. Korneev, and M. I. Elinson, *ibid.* 4, 267 (1966) [4, 179 (1966)]; Yu F. Ogrin, V. N. Lutskii, M. U. Arifova, V. I. Kovalev, V. B. Sandomirskii, and M. I. Elinson, Zh. Eksperim. i Teor. Fiz. 53, 1218 (1967) [Sov. Phys. JETP 26, 714 (1968)]; V. P. Duggal and Raj Rup, J. Appl. Phys. 40, 492 (1969); Jong Min Lee *et al.*, J. Korean Phys. Soc. 3, 27 (1970); R. A. Hoffman and D. R. Frankl, Phys. Rev. B 3, 1825 (1971).

[2]I. M. Lifshitz and A. M. Kosevich, Izv. Akad. Nauk SSSR, Ser. Fiz. 19, 395 (1955) [Bull. Acad. Sci. USSR, Phys. Ser. 19, 353 (1955)].

[3]Y. H. Kao, R. D. Brown, and R. L. Hartman, Phys. Rev. 136, A858 (1964).

[4]N. Garcia, Y. H. Kao, and O. F. Kammerer, Thin Films (to be published).

[5]W. S. Boyle and G. E. Smith, Progr. Semicond. 7, 1 (1963).

[6]L. V. Iogansen, Zh. Eksperim. i Teor. Fiz. 50, 709 (1966) [Sov. Phys. JETP 23, 470 (1966)].

[7]V. B. Sandomirskii, Zh. Eksperim. i Teor. Fiz. 52, 158 (1967) [Sov. Phys. JETP 25, 101 (1967)].

[8]A. Paskin and A. D. Singh, Phys. Rev. 140, A1965 (1965).

[9]R. Zitter, Phys. Rev. 127, 1471 (1962).

[10]J. M. Ziman, *Principles of the Theory of Solids* (Cambridge U.P., New York, 1964).

[11]See, for example, a review by L. A. Falkovski, Usp. Fiz. Nauk 94, 3 (1968) [Sov. Phys. Usp. 11, 1 (1968)].

[12]Y. H. Kao (unpublished).

[13]A. N. Friedman and S. H. Koenig, IBM J. Res. Develop. 4, 158 (1960).

[14]V. Ya Demikhovskii and B. A. Tavger, Fiz. Tverd. Tela. 6, 960 (1964) [Sov. Phys. Solid State 6, 743 (1964)].

[15]A. N. Friedman, Phys. Rev. 159, 553 (1967); R. Hartman, *ibid.* 181, 1070 (1969); E. W. Fenton, J. P. Jan, A. Karlson, and R. Singer, *ibid.* 184, 663 (1969); V. Chopra, R. K. Ray, and S. M. Bhagat, Phys. Status Solidi 4(a), 205 (1971); H. D. Drew and U. Strom, Phys. Rev. Letters 25, 1755 (1970); F. C. Chen, Jay Kirschenbaum, and Y. H. Kao (unpublished).

PHYSICAL REVIEW B VOLUME 5, NUMBER 6 15 MARCH 1972

Longitudinal Magnetoresistance of Thin Metallic Films with Partially Specular Boundary Scattering

Yuan-Shun Way and Yi-Han Kao*

National Tsing Hua University, Hsinchu, Taiwan, Republic of China

(Received 11 January 1971)

The longitudinal magnetoresistance of a thin metal film has been calculated using Chambers's method. It is assumed that the electron Fermi surface as well as the bulk mean-free path are spherically symmetric. Contrary to previous work based on the assumption of wholly diffuse surface scattering, we consider that scattering of electrons at the boundaries is partially specular. Explicit magnetoresistance curves have been calculated by numerical integration. It is found that low-field magnetoresistance depends quite sensitively on the fraction of specularly reflected electrons at the boundaries (ϵ). The resistance may change an order of magnitude between $\epsilon = 0$ and $\epsilon = 0.9$ in contrast to the corresponding $\sim 10\%$ variations in surface impedance associated with the anomalous skin effect. It is proposed that direct comparison between experimental data and the computed curves will yield information on the nature of boundary scattering.

I. INTRODUCTION

The behavior of free electrons in thin metallic films has been a subject of long-standing experimental and theoretical interest.[1] Owing to the presence of boundary scattering, the dynamics of conduction electrons in these films will differ significantly from that in the bulk material when the electronic mean-free path (mfp) becomes comparable to the film thickness. The first rigorous

theoretical treatment of this problem was given by Fuchs,[2] whose paper has formed the basis for almost all subsequent development.

The magnetoresistance of conductors with dimensions comparable to the electronic mfp is bound to be more complex than that of bulk samples because of the boundary-limited orbits. An excellent summary of earlier work on the calculations of the magnetoresistance of "thin" conductors has been given by Sondheimer.[3] The geometry-dependent magnetoresistance is quite a complicated computational problem, even considering the simplest case of a longitudinal magnetic field in a thin film. Previous calculations of the thin-film longitudinal magnetoresistance have been given by Koenigsberg,[4] Azbel,[5] Kaner,[6] Barron and McDonald,[7] Kao,[8] and most recently by McGill.[9]

The size dependence of the magnetoresistance, sometimes referred to as the magnetomorphic effect (MME), provides us with a useful means for determining the electronic mfp in metals as well as the nature of boundary scattering; both are of fundamental importance in our understanding of solids. It is therefore of interest to carry out computations of the MME subject to various boundary-scattering conditions so that a comparison between theory and experiment will yield information on the electronic structure in metallic films.

In a previous work,[8] detailed results were obtained by numerical integration. It has been shown that the longitudinal magnetoresistance increases with magnetic field H in the low-field region, undergoes a maximum, and eventually decreases with H in the high-field regime. It was pointed out in this paper that this maximum may be employed to obtain information on the electronic mfp and cyclotron radius. However, in this calculation as well as other work on thin films in a longitudinal field, it was assumed that scattering at the boundaries is wholly diffuse. One is unable to learn about the nature of boundary scattering by comparing experimental results with these theories.

The present paper is concerned with the calculation of longitudinal magnetoresistance of thin films when the boundary scattering is allowed to be partially specular. As our results will show, the magnetoresistance curve together with the shape and position of the maximum mentioned above indeed depend on the extent of specular reflection at the boundaries. A comparison between experimental results and the present theory should allow us to extract information on the nature of boundary scattering.

II. LONGITUDINAL MAGNETORESISTANCE OF THIN FILMS

A. Basic Equations

For the sake of simplicity, we consider as usual the case of a free-electron gas confined in the space bounded by the planes $y = 0$ and $y = d$. The bulk mfp l and effective mass m^* of electrons are assumed to be isotropic. Following Chambers's method,[10] we may write the size-dependent conductivity as

$$\sigma = \frac{3\sigma_0}{4\pi S}\int dS \int d\phi \int d\theta \sin\theta \cos^2\theta \times \left[1 - \frac{(1-\epsilon)e^{-PO/l}}{1-\epsilon e^{-PP'/l}}\right], \quad (1)$$

where σ_0 is the bulk conductivity, S the cross-sectional area of the specimen perpendicular to the current, and ϵ is the fraction of electrons suffering specular reflection at the boundaries. PO is the path length of an electron trajectory from a point P on the boundary to a point O inside the film, PP' is the path length of a trajectory between two points P and P' on opposite boundaries. The trajectories in zero magnetic field are shown in Fig. 1(a). The integral on S averages the contributions to σ at all points like O. It is worth noting that in the isotropic case considered here, by following the trajectory of a given electron, all the paths PP' are of the same length.

In the presence of a longitudinal magnetic field, which produces no drift current but modifies the electron trajectories, Eq. (1) is still applicable provided PO and PP' are now measured along the spiral trajectories of electrons under the influence of H. This is illustrated in Figs. 1(b) and 1(c). Note that because of the symmetry in the problem, all the curved paths PP' are still of the same length. Based on this observation, we may carry out the calculations following a trajectory analysis similar to those given in Ref. 8. Equation (1) can be extended to the case with anisotropic Fermi surfaces by a straightforward but tedious modification of the terms in square brackets in (1).

Following the formalism and notations used in Ref. 8 (hereafter to be referred to as I), we rewrite the equation for the conductivity in the presence of a longitudinal magnetic field as

$$\frac{\sigma}{\sigma_0} = 1 - \frac{3(1-\epsilon)}{4\pi d}\int d\theta \sin\theta \cos^2\theta \times \int dy \int d\phi \frac{e^{-\psi(y,\phi,\theta)/\eta}}{1-\epsilon e^{-\Psi(y,\phi,\theta)/\eta}}, \quad (2)$$

where $\eta = l/r_0$ and $r_0 = m^* vc/eH$. Other quantities used in (2) are illustrated in Fig. 2, $r = r_0 \sin\theta$, θ is the angle between the z axis ($z \parallel H \parallel E$) and the tangent to an electron trajectory at point O, ψ is the angle which the projection of an electron on the x-y plane traverses on a circle of radius r from a point P on the lower boundary to a general point O in the interior of the film, and Ψ is the

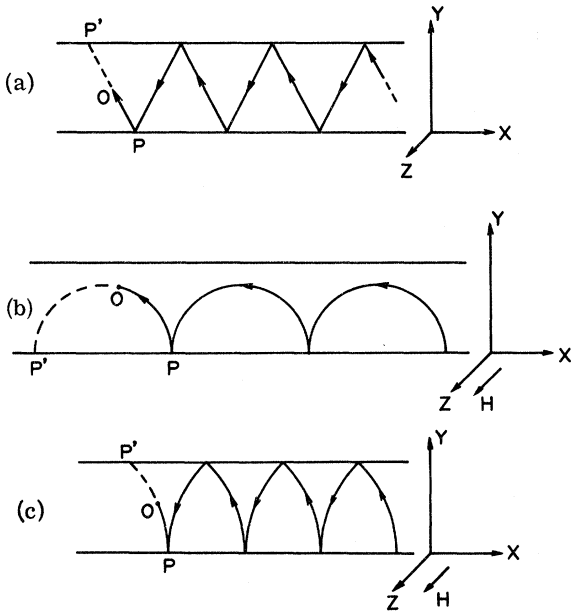

FIG. 1. Typical electron trajectories in thin conducting films with partially specular reflection at the boundaries: (a) in the absence of H; (b) in a longitudinal H but electrons only collide with one boundary; (c) electrons collide with both boundaries in a longitudinal H.

angle this projection point would have traversed around the same circle if the circular arc PO were extended until it meets with a boundary. For a given H and θ, once the point O at (y, ϕ) is chosen on the x-y plane, there are uniquely defined $\psi(y, \phi, \theta)$ and $\Psi(y, \phi, \theta)$ such that $\psi/\eta = \text{arc}(PO)/l$ and $\Psi/\eta = \text{arc}(PP')/l$.

B. Orbit Analysis

We proceed to compute the integral in (2) by finding explicit expressions for ψ and Ψ. These expressions can be readily obtained by an analysis of the orbits with the aid of Fig. 3. We distinguish between two separate cases: (a) PP' intersects both boundary planes [Fig. 3(a)] and (b) PP' intersects only one plane $y = 0$ [Fig. 3(b)]. Orbits of case (b) are often called "skipping orbits." In Figs. 3(a) and 3(b), the points B, Q, and B' are projections of P, O, and P' on the x-y plane, respectively. For simplicity, we have always considered orbits originating from the point P on the lower boundary $y = 0$. The final result should be independent of the direction of H and, by symmetry consideration, orbits originating from the upper boundary $y = d$ must give equal contributions as those from the lower boundary. Consequently, we now only consider the situation when P is on $y = 0$ and shall eventually multiply the result by 2 to account for the total contribution by electrons scattered from both boundaries.

Case (a). P on $y = 0$ and P' on $y = d$ [Fig. 3(a)]:

$$\phi = \psi + \psi_0, \quad \beta = \tfrac{1}{2}\pi - \psi_0, \quad \sin\beta = \frac{(y + r\cos\phi)}{r},$$

and hence

$$\psi = \phi + \arcsin\left(\frac{y}{r} + \cos\phi\right) - \tfrac{1}{2}\pi, \tag{3}$$

$$\Psi = \arcsin\left(\frac{y}{r} + \cos\phi\right) + \arcsin\left(\frac{d}{r} - \frac{y}{r} - \cos\phi\right). \tag{4}$$

Case(b). Both P and P' fall on $y = 0$ [Fig. 3(b)]:

$$\phi = \psi + \psi_0, \quad \beta = \psi_0 - \tfrac{1}{2}\pi, \quad \sin\beta = -(y + r\cos\phi)/r,$$

and hence

$$\psi = \phi + \arcsin\left(\frac{y}{r} + \cos\phi\right) - \tfrac{1}{2}\pi, \tag{5}$$

$$\Psi = \pi + 2\arcsin\left(\frac{y}{r} + \cos\phi\right). \tag{6}$$

Note that the expression for ψ is the same for both cases. For a fixed y and r, whether P' will fall on the upper plane $y = d$ or the lower plane $y = 0$ depends the value of ϕ at Q. If $y + r(1 + \cos\phi)$

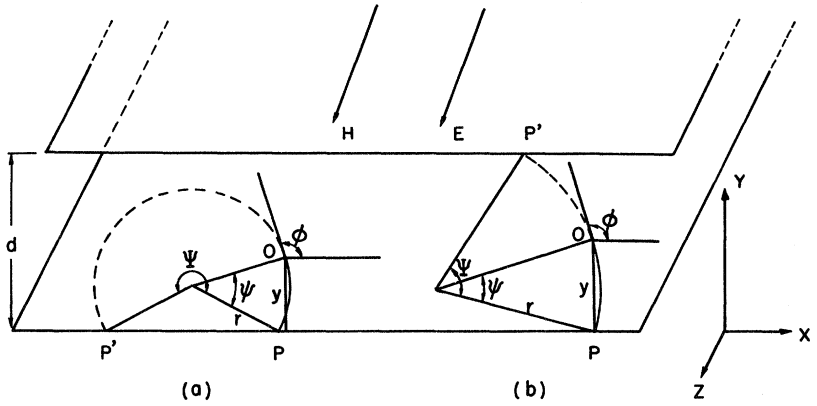

FIG. 2. The geometry of the thin film and the applied fields: (a) orbit intersects one boundary; (b) orbit intersects both boundaries.

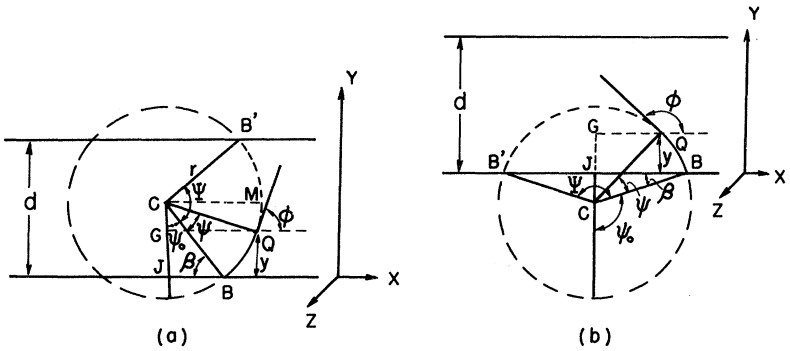

FIG. 3. Construction for the determination of ψ and Ψ. (a) Orbit intersects both boundaries [case (a)]. (b) Orbit intersects only one boundary [case (b)].

$\geq d$, the orbit will intersect the upper plane and (4) shall be used for Ψ[case (a)]. If $y + r(1+\cos\phi) < d$, the orbit will miss $y = d$ and P' will land on $y = 0$. Equation (6) will be used for Ψ [case (b)].

For a given r and a fixed y for the point Q in Figs. 3, ϕ is allowed only in a limited range. The limits can be found by drawing circles on the projection (x-y) plane just touching the lower boundary $y = 0$ (Figs. 4). From Fig. 4(a) we find $\phi_{min} = \frac{1}{2}\pi - \arcsin(1 - y/r)$, and from Fig. 4(b) we obtain $\phi_{max} = \frac{3}{2}\pi + \arcsin(1 - y/r)$. However, as we shall carry out the integral on ϕ first, the upper limit will be ϕ_{max} only for case (b). For case (a), when the electron-orbit intersects both boundary planes, the upper limit must be replaced by ϕ_c, the critical angle obtained by drawing a circle touching $y = d$ and going through the point Q on the x-y plane (Fig. 5). From this figure, we obtain $\phi_c = \frac{1}{2}\pi - \arcsin(d/r - y/r - 1)$.

Using the results given in (3)–(6) and the integration limits as discussed above, we arrive at the final expression for the magnetoconductivity:

$$\frac{\sigma}{\sigma_0} = 1 - 2\times\frac{3(1-\epsilon)}{4\pi}\int_0^{\pi} d\theta \sin\theta\cos^2\theta \int_0^{1+(2\mu\sin\theta-1)\Theta(1-2\mu\sin\theta)} d\xi\,(I_a + I_b)\,, \tag{7}$$

where

$$I_a = \int_{\phi_{min}}^{\phi_c} d\phi\, \frac{\exp\{-\mu\alpha[\phi + \arcsin(\xi/\mu\sin\theta + \cos\phi) - \frac{1}{2}\pi]\}[1 - \Theta(1 - \xi - \mu\sin\theta - \mu\sin\theta\cos\phi)]}{1 - \epsilon\exp\{-\mu\alpha[\arcsin(\xi/\mu\sin\theta + \cos\phi) + \arcsin(1/\mu\sin\theta - \xi/\mu\sin\theta - \cos\phi)]\}}\,, \tag{8}$$

$$I_b = \int_{\phi_{min}}^{\phi_{max}} d\phi\, \frac{\exp\{-\mu\alpha[\phi + \arcsin(\xi/\mu\sin\theta + \cos\phi) - \frac{1}{2}\pi]\}\Theta(1 - \xi - \mu\sin\theta - \mu\sin\theta\cos\phi)}{1 - \epsilon\exp\{-\mu\alpha[\pi + 2\arcsin(\xi/\mu\sin\theta + \cos\phi)]\}}\,, \tag{9}$$

$\Theta(x) = 1, \quad x > 0$
$\quad\;\; = 0, \quad x < 0$

$\xi = y/d$, $\alpha = d/l$, and $\mu = r_0/d = m^* vc/eHd$.

The factor 2 appearing in front of the integrals in (7) takes account of electrons scattered from both boundaries $y = 0$ and $y = d$. The integral I_a [Eq. (8)] accounts for the orbits of case (a) and

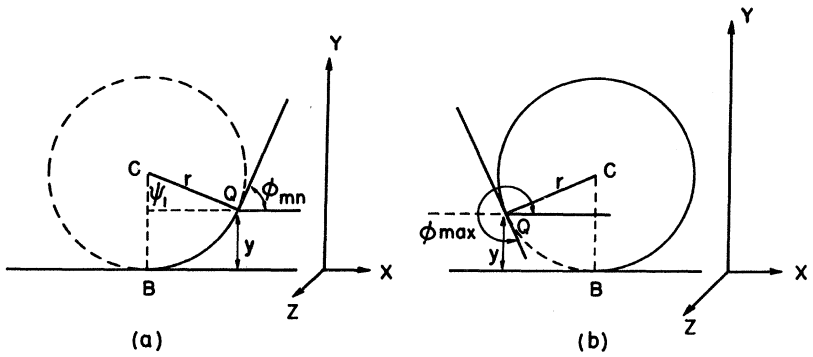

FIG. 4. Construction for the determination of allowed range of ϕ: (a) lower limit ϕ_{min}; (b) upper limit ϕ_{max}.

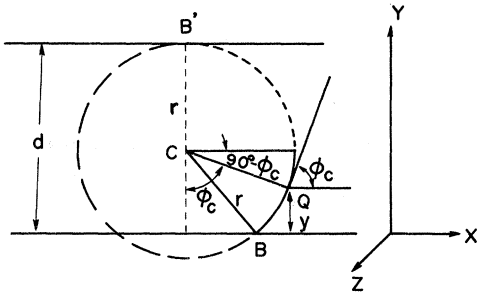

FIG. 5. Construction for the determination of the critical value of ϕ in case (a).

I_b[Eq. (9)] accounts for those of case (b).

III. RESULTS AND DISCUSSION

The integrals in (7)–(9) have been computed by the method of Gaussian quadrature using CDC-3300 and IBM-1130 computers. The magnetoresistance curves for $\alpha = 0.1$ and 0.01 are shown in Figs. 6 and 7 ($\rho = \sigma^{-1}$, ρ_0 is the field-independent bulk resistivity). Some characteristic numbers are listed in Tables I and II.

The curves for completely diffuse scattering at boundaries are the same as those computed in I. Introducing partially specular boundary scattering leads to lower resistance, and the resistance maximum becomes less pronounced. As expected, the resistance for totally specular boundary scattering ($\epsilon = 1$) is independent of H. Changing the boundary condition from $\epsilon = 0$ to $\epsilon = 0.9$ gives rise to a decrease in the resistance at maximum by a factor of ~4.5 for $\alpha = 0.1$ and by a factor of ~10 for $\alpha = 0.01$. Thus, using the dc magnetoresistance one is able to observe sizable variations due to boundary scattering in contrast to the small changes encountered in the anomalous skin effect[11] (in which the surface impedance changes by ~10% between $\epsilon = 0$ and $\epsilon = 1$).

It is hoped that the calculated curves, as those shown in Figs. 6 and 7, can be used for a direct comparison between experimental data and theoretical predictions. Because of the sensitive dependence of the resistance values on the boundary diffuseness in the low-field region, this method can be conveniently used to obtain the parameter ϵ. Curves shown in Figs. 6 and 7 can be readily applied to metals having nearly spherical Fermi surface with small bulk magnetoresistance (such as the alkalis). Metals having more complicated Fermi surfaces but with a nearly isotropic mfp can be accounted for, in principle, by appropriate modifications of the orbits used for evaluating the integrals in (7). Metals with anisotropic mfp will be difficult to handle by the present approach since electrons moving in different directions all contribute to the film resistance. To determine the anisotropic mfp, more selective methods will have to be used.

Care has to be taken in making a comparison between the theoretical and experimental curves. The ρ vs H curves with low α and high ϵ may look much like the curves with higher α but lower ϵ. For example, $\alpha = 0.01$, $\epsilon = 0.9$ (curve j, Fig. 7) and $\alpha = 0.1$, $\epsilon = 0.3$ (curve d, Fig. 6) may give rise to quite similar magnetoresistance in the region near the resistivity maximum. Without discriminating these similar cases, it is difficult to identify the parameter ϵ and the mfp l unequivocally. This fact may account for some ambiguities in the values of ϵ determined by this method found in the literature.

In order to determine ϵ with reasonable accuracy by the present method, information on the bulk mfp l obtained from experiments making no use of the surface scattering (such as damping of electro-

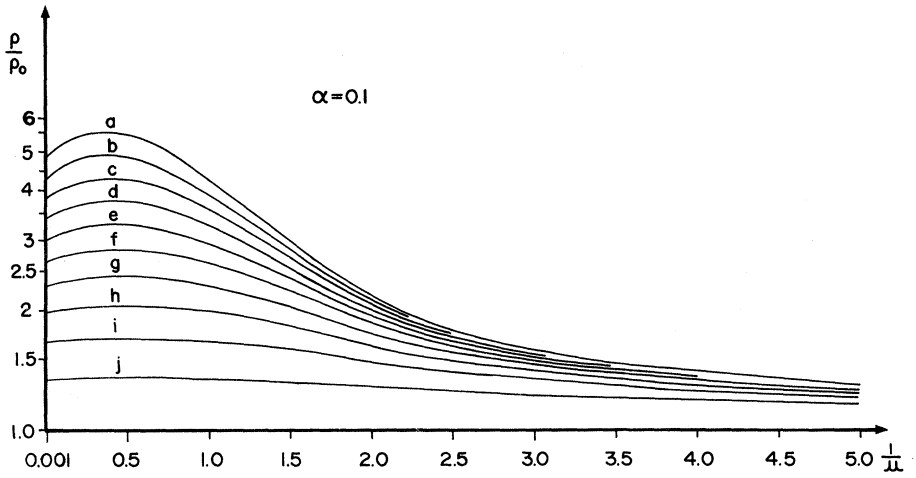

FIG. 6. Computed longitudinal magnetoresistance curves (ρ/ρ_0 vs $1/\mu = deH/m^*vc$) for $\alpha = d/l = 0.1$. ϵ values: 0(a), 0.1(b), 0.2(c), 0.3(d), 0.4(e), 0.5(f), 0.6(g), 0.7(h), 0.8(i), 0.9(j). See also Table I.

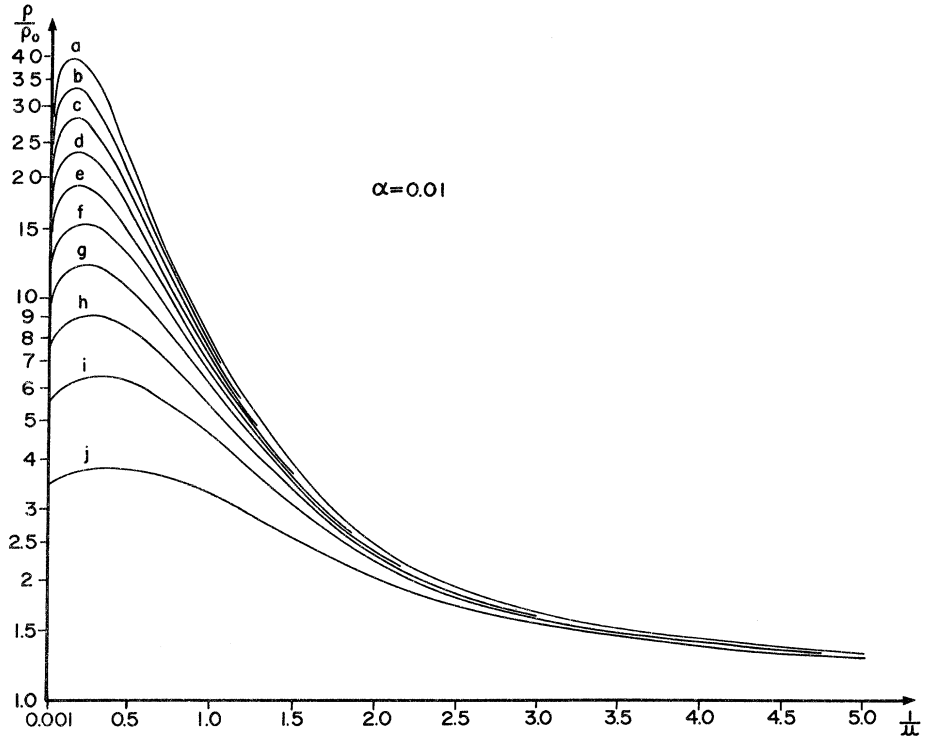

FIG. 7. Computed longitudinal magnetoresistance curves for $\alpha = d/l = 0.01$. ϵ values: 0(a), 0.1(b), 0.2(c), 0.3(d), 0.4(e), 0.5(f), 0.6(g), 0.7(h), 0.8(i), 0.9(j). See also Table II.

magnetic waves, broadening of absorption lines, etc.) will be very helpful.

From the computed curves in Figs. 6 and 7, we found that the position where the resistivity maximum occurs moves slightly towards the high-field side as ϵ increases. The maximum also "broadens" in increasing ϵ. When ϵ is close to unity the maximum becomes ill defined and identifying its location for $\epsilon \lesssim 1$ is probably of little value. We feel that the occurrence of such a maximum should mainly serve the purpose for identifying the gross feature of this special effect rather than to be used for accurate measurements. Quantitative determination of cyclotron radius or mfp can be made only when both α and ϵ are small enough. Moreover, it is believed that in metals with anisotropic Fermi surfaces, the position as well as the "line shape" of this maximum will depend largely on the anisotropy.

The results shown in Figs. 6 and 7 are mainly concerned with the occurrence of a resistivity maximum and its variation with ϵ. It is, however, useful to compare the asymptotic behavior of these magnetoresistance curves by numerical calculation

TABLE I. Characteristic values of curves shown in Fig. 6, $\alpha = 0.1$.

Identification	ϵ	ρ/ρ_0 $1/\mu = 0.001$	ρ/ρ_0 $1/\mu = 5$	ρ/ρ_0 at ρ_{max}	Approximate location $(1/\mu)$ of ρ_{max}
a	0	4.796	1.294	5.596	0.35
b	0.1	4.297	1.291	4.905	0.35
c	0.2	3.841	1.287	4.298	0.40
d	0.3	3.423	1.283	3.759	0.40
e	0.4	3.035	1.277	3.274	0.45
f	0.5	2.674	1.269	2.835	0.45
g	0.6	2.327	1.258	2.430	0.45
h	0.7	1.997	1.242	2.055	0.50
i	0.8	1.674	1.216	1.699	0.50
j	0.9	1.349	1.164	1.354	0.50

TABLE II. Characteristic values of curves shown in Fig. 7, $\alpha = 0.01$.

Identification	ϵ	ρ/ρ_0 $1/\mu = 0.001$	ρ/ρ_0 $1/\mu = 5$	ρ/ρ_0 at ρ_{max}	Approximate location $(1/\mu)$ of ρ_{max}
a	0	28.26	1.307	39.68	0.1
b	0.1	24.09	1.307	33.28	0.15
c	0.2	20.49	1.306	27.89	0.15
d	0.3	17.34	1.306	23.17	0.15
e	0.4	14.55	1.305	19.01	0.15
f	0.5	12.03	1.304	15.40	0.20
g	0.6	9.724	1.302	12.12	0.20
h	0.7	7.581	1.300	9.159	0.25
i	0.8	5.533	1.295	6.412	0.30
j	0.9	3.482	1.282	3.798	0.40

with those obtained by analytical methds. We first note that the effect of including the possibility of partially specular boundary scattering lies in the appearance of two terms containing ϵ in the general expression Eq. (2). But analytical expressions for the present problem with $\epsilon \neq 0$ do not seem to exist in the literature. We shall therefore only compare the limiting cases for $\epsilon = 0$.

For high-magnetic fields $d \gg 2r_0$, our results indicate that ρ/ρ_0 varies as μ, or the magnetoresistance goes as $1/H$. This is in accord with the asymptotic expressions obtained by Koenigsberg,[4] Azbel,[5] and Kaner.[6] In fact, by noting $y = r\cos(\phi - \psi) - r\cos\phi$ and changing the integral on y to ψ, one may easily carry out the integrations in (2) (setting ϵ to zero for simplicity) and obtain for the high-field limit

$$\frac{\sigma}{\sigma_0} = 1 - \frac{3}{8\alpha}\left(1 - \frac{1 + e^{-2\pi/\eta}}{2(1 + 4\eta^{-2})}\right), \tag{10}$$

which gives $\rho/\rho_0 \simeq 1 + 3\pi\mu/8$ for $\eta (= l/r_0) \gg 1$.

For low magnetic fields $d \ll 2r_0$, the situation becomes more complicated, and it is hardly possible to obtain an exact asymptotic field dependence from the general expression [such as Eq. (7)] without going into detailed orbit analysis. Using an order-of-magnitude estimate, Azbel[5] has shown that a maximum in the longitudinal magnetoresistance should exist near $r \sim (ld)^{1/2}$ and a "negative magnetoresistance" with $\rho \sim A - BH^2$ should occur near $r \sim l^2/d$, i.e., a maximum near $1/\mu \sim \alpha^{1/2}$ (which is in agreement with the numerical results of Ref. 8) and $\rho \sim A - BH^2$ near $1/\mu \sim \alpha^2$. For the same problem, Kaner[6] obtained from the transport equation that a region with $\rho \sim H^2$ may occur with $r \gg l^2/d$ and $d \ll r$ (or $1/\mu \ll \alpha^2$).

It should be noted that these H^2-dependent regions in low fields must be due to a weak effect since the main contribution should arise from a small number of effective electrons. Moreover, they should occur in a very narrow field region.[5] As was mentioned before, our present work is mainly devoted to the calculation of the magnetoresistance near the maximum; from the calculated values at rather large intervals of $1/\mu$ [$\Delta(1/\mu) = 0.05$], which we used to construct Figs. 6 and 7, the H^2 dependence does not appear. For $\alpha = 0.01$, the H^2 region should occur near $1/\mu = 0.0001$, much below the lowest $1/\mu$ value (0.001) we have used. For $\alpha = 0.1$, the H^2 dependence may occur around $1/\mu = 0.01$, but much finer steps in $1/\mu$ must be used in the numerical work. Furthermore, much higher accuracy will be required to search for such a weak effect.

Our computed values at $1/\mu = 0.001$ are close to the zero-field resistivity values obtained by Sondheimer.[3] A comparison between our values at $1/\mu = 0.001$, with $\epsilon = 0$ and $\epsilon = 0.5$ with those given by Sondheimer at $H = 0$ shows a difference of at worst a few percent. This close agreement also supports the conjecture that the H^2 dependence, if present, must be a weak effect unless some drastic variation should occur in a very narrow field region.

To date, the maximum in longitudinal magnetoresistance of thin films has been observed in Sb by Steele,[12] in Bi by Babiskin[13] and by Friedman and Koenig,[14] in In by Olsen,[15] de la Cruz *et al.*,[16] in Au, Ag, In, and Al by Chopra,[17] in Zn by Gaidukov and Kadletsova,[18] and in Al by Rau.[19] The comparison between theoretical predictions and experimental results has met with good agreement in certain metals while in some cases it was less successful. Three factors are believed to be responsible for the unsuccessful situations. First, the bulk magnetoresistance is normally quite large for metals with long l and anisotropic Fermi surfaces except for very few alkali metals. In order to extract the size-effect contribution, better methods for subtracting the bulk contributions from the measured thin-film magnetoresistance or more accurate computation of these contributions (including Shubnikov–de Haas quantum effect in certain metals) will have to be pursued. Second, as mentioned above, the anisotropy in either the Fermi surface or the mfp l may give rise to not only a sizable change of the shape but also a possible shift of the position of the resistance maximum. To resolve this complexity, a different transport approach will probably be necessary. Third, the present-day understanding of the boundary scattering of electrons is still primitive. Most of the time we simply assume that the boundary scattering can be represented by a single parameter ϵ; this is by no means justified. Although more complicated boundary conditions have been suggested,[20] computations have indicated that these modified conditions do not necessarily lead to better agreement with experimental data.[21] It is hoped that the present approach will serve the purpose of finding some qualitative features of the surface scattering and, based upon this information, more detailed and quantitative approaches can be taken to unravel the whole problem of surface potentials and boundary scattering.

IV. CONCLUSION

We have extended a previous work on thin-film longitudinal magnetoresistance based on wholly diffuse surface scattering to the more general situation when the surface scattering is allowed to be partially specular. It is hoped that in the cases where the size-effect magnetoresistance can be extracted out of an experimental total-longitudinal-magnetoresistance curve, a comparison between these data with the computed curves will provide

us an effective means of studying the nature of boundary scattering of conduction electrons.

ACKNOWLEDGMENTS

We are indebted to the staff of the Computing Center at Tsing Hua University for their assistance in numerical work. One of us (Y.H.K.) would like to thank the members of the Institute of Physics at Tsing Hua for the hospitality extended to him during his sabbatical leave.

*Permanent address: Department of Physics, State University of New York, Stony Brook, N. Y. 11790.

[1]For a recent review, see for example, R. G. Chambers, in *The Physics of Metals*, Vol. I, edited by J. M. Ziman (Cambridge U. P., New York, 1969).

[2]K. Fuchs, Proc. Cambridge Phil. Soc. 34, 100 (1938).

[3]E. H. Sondheimer, Advan. Phys. 1, 1 (1952).

[4]E. Koenigsberg, Phys. Rev. 91, 8 (1953).

[5]M. Ya. Azbel, Dokl. Akad. Nauk SSSR 99, 519 (1954); Zh. Eksperim. i Teor. Fiz. 44, 1262 (1963) [Sov. Phys. JETP 17, 851 (1963)].

[6]E. A. Kaner, Zh. Eksperim. i Teor. Fiz. 34, 658 (1958) [Sov. Phys. JETP 7, 454 (1958)].

[7]T. H. K. Barron and D. K. C. McDonald, Physica 24, S102 (1958).

[8]Y. H. Kao, Phys. Rev. 138, A1412 (1965).

[9]N. C. McGill, Physica 40, 91 (1968).

[10]R. G. Chambers, Proc. Roy. Soc. (London) A202, 378 (1950).

[11]G. E. Reuter and E. H. Sondheimer, Proc. Roy. Soc. (London) A195, 336 (1949).

[12]M. C. Steele, Phys. Rev. 97, 1720 (1955).

[13]J. Babiskin, Phys. Rev. 107, 981 (1957).

[14]A. N. Friedman and S. H. Koenig, IBM J. Res. Develop. 4, 158 (1960).

[15]J. L. Olsen, Helv. Phys. Acta 31, 713 (1958).

[16]M. E. de la Cruz, F. de la Cruz, and J. M. Cotignola (private communication); and Phys. Rev. 163, 575 (1967).

[17]K. L. Chopra, Phys. Rev. 155, 660 (1967).

[18]Yu. P. Gaidukov and Ya. Kadletsova, Zh. Eksperim. i Teor. Fiz. Pis'ma v Redaktsiyu 8, 247 (1968) [Sov. Phys. JETP Letters 8, 151 (1968)].

[19]C. Rau (private communication).

[20]J. E. Parrott, Proc. Phys. Soc. (London) 85, 1143 (1965).

[21]C. S. Lee and Y. H. Kao (unpublished).

PHYSICAL REVIEW B VOLUME 5, NUMBER 6 15 MARCH 1972

Anisotropy of the Threshold Energy for the Production of Frenkel Pairs in Tantalum

Peter Jung and Werner Schilling
Institut für Festkörperforschung, Kernforschungsanlage Jülich, 517 Jülich, Germany
(Received 14 September 1971)

Thin tantalum single-crystal foils with the ⟨110⟩ direction normal to the surface have been irradiated with electrons of energies between 1.0 to 3.2 MeV. By varying the orientation of the foil relative to the direction of the beam over a major part of the fundamental triangle, a strong directional effect in the damage rate was observed for transferred energies of more than 36 eV. In previous measurements especially on the fcc metals copper and gold, much less, if any, anisotropy of the defect production was observed. The data have been corrected for beam spreading due to the finite sample thickness. From the dependence of the defect production on electron energy and foil orientation, the angular dependence of the threshold displacement energy could be fitted. Good over-all fits were only possible when the averaged threshold was about 36 eV in a region of 20° around the ⟨111⟩ direction, about 53 eV in a region of 18° around the ⟨100⟩ direction, and larger than 130 eV in other directions. The existence of such "windows" along the close-packed directions indicates a sequence of replacement collisions which eventually leads to a stable defect. Computer calculations by the Brookhaven group for bcc iron yielded similar threshold windows around the principal crystallographic directions. However, the ratio of the threshold values for the ⟨100⟩ and ⟨111⟩ directions obtained by this group does not agree with our result. For the lowest threshold energy in tantalum, we found 32 ± 2 eV, and for the electrical resistivity per unity concentration of Frenkel pairs, we obtained $(17 \pm 3) \times 10^{-4}$ Ω cm.

I. INTRODUCTION

Irradiation of a crystal with fast electrons results in a transfer of recoil energy to the lattice atoms. If this recoil energy exceeds a certain threshold value T_d, the struck atom can be displaced permanently from its lattice site, leaving behind a vacancy. Besides this vacancy, an interstitial is produced at some distance via replacement collisions. The interstitial together with the vacancy is called a Frenkel pair.

The atomic structure of the lattice causes the threshold energy to depend on the direction of the knocked-on atom. Therefore, in single-crystal